

Inversion of Venus internal structure based on geodetic data

Chi Xiao¹, Fei Li^{*1,2}, Jian-Guo Yan^{*2}, Wei-Feng Hao¹, Yuji Harada³, Mao Ye² and Jean-Pierre Barriot⁴

¹ Chinese Antarctic Center of Surveying and Mapping, Wuhan University, Wuhan 430079, China

² State Key Laboratory of Information Engineering in Surveying, Mapping and Remote Sensing, Wuhan University, Wuhan 430079, China; fli@whu.edu.cn, jgyan@whu.edu.cn

³ Space Science Institute, Macau University of Science and Technology, Avenida Wailong, Taipa, Macau, China

⁴ Observatory Geodetic de Tahiti, BP 6570, 98702 Faa'a, Tahiti, French Polynesia

Received 2018 December 12; accepted 2020 March 12

Abstract Understanding the internal structure of Venus promotes the exploration of the evolutionary history of this planet. However, the existing research concerning the internal structure of Venus has not used any inversion methods. In this work we employed an inversion method to determine the internal structure of Venus using observational or hypothetical geodetic data; these data include mass, mean radius, mean moment of inertia and second degree tidal Love number k_2 . To determine the core state of Venus, we created two models of Venus, an isotropic 3-layer model with entire liquid core and an isotropic 4-layer model with liquid outer core and a solid inner core, assuming that the interior of Venus is spherically symmetric and in hydrostatic equilibrium. A series of the sensitivity analysis of interior structure parameters to the geodetic data considered in here shows that not all of the parameters can be constrained by the geodetic data from Venus. On this basis, a Markov Chain Monte Carlo algorithm was used to determine the posterior probability distribution and the optimal values of the internal structure parameters of Venus with the geodetic data. We found that the 3-layer model is more credible than the 4-layer model via currently geodetic data. For the assumption of the 3-layer model with the $k_2 = 0.295 \pm 0.066$, $I/MR^2 = 0.33 \pm 0.0165$, and $\bar{\rho} = 5242.7 \pm 2.6 \text{ kg m}^{-3}$, the liquid iron-rich core of Venus has a radius of 3294_{-261}^{+215} km, which suggests a larger core than previous research has indicated. The average density of the mantle and liquid core of Venus are 4101_{-375}^{+325} and 11885_{-1242}^{+955} kg m^{-3} , respectively.

Key words: planets and satellites: interiors — planets and satellites: terrestrial planets — planets and satellites: physical evolution — planets and satellites: fundamental parameters

1 INTRODUCTION

Venus was once considered to be Earth's sister planet because of the similarity in mass and radius and their close proximity in the Solar system. Therefore, the initial knowledge about the internal structure of Venus was based on the understanding of the interior of Earth. Early research assumed that Venus, like Earth, consisted of a solid inner core, liquid outer core, viscoelastic solid mantle, and solid crust. Tremendous differences between the surface of Venus and Earth have been discovered since the beginning of Venus exploration missions, such as Venera 9 (which was the first lander that returned images from the surface of Venus). Venera 9 also collected data about pressure, temperature, wind velocity and material composition on the

surface of Venus (Florensky et al. 1977), and changed our understanding of this planet. Carbon dioxide with a content of about 96% dominates the atmosphere of Venus and the surface temperature of Venus is about 730 K (Taylor 1985), which are significantly different from Earth. Moreover, Venus lacks the plate tectonics (Spohn et al. 2014) found on Earth. These observations indicate that the interior thermal activity and evolution history of Venus is different from Earth. The understanding of its internal structure is a crucial foundation to explore the origin and evolution of Venus.

In the past few decades, many different methods have been applied to study the internal structure of Venus. Grimm & Solomon (1988) used radar altimetry data and topography of impact craters from Venera 15/16 to infer Venus's crustal thickness and found that this value was in

* Corresponding author

the range from 10 to 20 km with a density of 2900 kg m^{-3} . Geoid-to-topography ratios were used in recent research to determine the crustal thickness of Venus. Applying this method, James et al. (2010) inferred the crustal thickness as 30 km. Yang et al. (2016) estimated this value to be about 25 km. Buck (1992) determined the crustal viscosity of Venus to be at least 10^{18} Pa s by using geoid and topography data; the crustal viscosity of Earth was considered to be $10^{19} - 10^{26} \text{ Pa s}$ (Bills et al. 1994), for comparison. However, these methods and data are unable to constrain the mantle and core of Venus.

Among the various geophysical approaches, seismology may be the most suitable method for determining the internal structure of planets. Unlike the Passive Seismic Experiment (PSE) that was executed during the Apollo mission to the Moon, the seismic data collected by Venera 13 and 14 (Ksanfomaliti et al. 1982) which received by only a single seismic station, were insufficient for inferring the internal structure of Venus (Knapmeyer 2011). Thus, there were only hypothetical models of the internal structure of Venus. In the Basaltic Volcanism Study Project (Basaltic Volcanism Study Project 1981), the density of the core of Venus was considered to be about 9800 kg m^{-3} , and the core radius was determined to be 3252 km. Steinberger et al. (2010) used gravity anomalies and topography to estimate the density of the upper mantle to be 3378 kg m^{-3} . They also inferred the core radius to be about 3186 km with a mantle viscosity of $10^{20} - 10^{23} \text{ Pa s}$. Parmentier & Hess (1992) estimated the viscosity of a mantle of Venus as $0.5 \times 10^{21} - 1 \times 10^{21} \text{ Pa s}$ using a geochemical method. Huang et al. (2013) studied Venus's mantle convection models by numerical simulation, and found that average mantle viscosity of $2 \times 10^{21} \text{ Pa s}$ is consistent with present observations of Venus, including the volcanism, topography, and gravity. Aitta (2012) used the empirical relation between density and pressure to build the mantle model, applying tricritical phenomena theory (Aitta 2010) to constrain the liquid core. These results indicated that the average densities of mantle and core of Venus to be 4600 and 10600 kg m^{-3} , respectively, with a core radius of 3228 km, although, the core state of Venus was not well determined.

To determine the core state of Venus, the tidal response was introduced into studies. Venus is deformed by the tidal force of other celestial bodies, such as the Sun. This tidal deformation reflects the rheological parameters of Venus expressed by three dimensionless Love numbers: k , l , and h . Yoder (1995) used a series of models whose parameters were fixed to calculate the theoretical second degree tidal Love number k_2 of Venus. Yoder found that if Venus has a solid iron-rich core, the synthetic k_2 is about 0.17; and this k_2 would range from 0.23 to 0.29 for a liquid iron core.

Using Doppler tracking from the Magellan and Pioneer Venus Orbiter (PVO) spacecraft data, Konopliv & Yoder (1996) estimated that the value of k_2 is $0.295 \pm 0.066 (2\sigma)$. Dumoulin et al. (2017) also constructed six models based on different chemical composition to calculate the synthetic tidal Love number k_2 . In their study, a k_2 value larger than 0.27 indicated a partially or entirely liquid core. Thus, Venus quite likely has a liquid core instead of an entirely solid core. For the sake of simplicity, we call these ‘forward modeling methods’, which use models whose parameters are known to calculate the synthetic data, as opposed to inversion methods. The forward modeling method is not only applied to the studies of Venus but also widely used in the studies of other planets. With the help of the tidal Love number k_2 and tidal dissipation factor Q of the Moon, Harada et al. (2014), Harada et al. (2016), and Williams & Boggs (2015) found the evidence of the existence of a partially melting layer in the lunar lower mantle. Padovan et al. (2014) studied the relationship between the k_2 and the size and composition of the core of Mercury and provide evidence of the existence of a solid Fe-S layer at the top of the core of Mercury. Generally, the tidal Love number k_2 responds to the internal structure of planets, especially the lower mantle and core.

A combination of planetary geodetic parameters — including mass, mean radius, mean moment of inertia (MoI), and tidal Love number k_2 — have been employed to explore the mantle and core of the Moon and Mars (Matsumoto et al. 2015; Khan et al. 2018). Since the calculation of tidal Love number k_2 from model parameters, unlike calculating mass and mean MoI, is a non-linear process (see Appendix B), a Markov Chain Monte Carlo (MCMC) algorithm was introduced to address inversion problem. By using the MCMC algorithm, Matsumoto et al. (2015) inverted lunar interior structure to extract information about lunar core structure based on the k_2 , mean MoI, mean density, and seismic travel time. Khan et al. (2018) also used the MCMC algorithm to invert the Martian interior structure and composition based on k_2 , mean MoI, mean density, global tidal dissipation factor Q , and prior geochemical information. However, this method has not been applied to Venus.

Most research in the past addressing the internal structure of Venus has used the forward modeling method (e.g., Yoder 1995; Aitta 2012; Dumoulin et al. 2017), but none of the existing research is considered the inversion method. Only a limited number of internal structure models were studied with the help of the forward modeling method. The inversion method is necessary to understand the internal structure of Venus further. To fill this gap, this paper uses the MCMC algorithm to invert the internal structure of Venus with its geodetic data. The rest of this

Table 1 The Geodetic Data of Venus

Parameter	Symbol	Value
Mean radius	R	$6051.8 \pm 1 \text{ km}$
Standard gravitational	GM	$324858.592 \pm 0.006 \times 10^9 \text{ m}^3\text{s}^{-2}$
Mean MoI	I/MR^2	~ 0.33
Tidal Love number	k_2	0.295 ± 0.066
Mean density	$\bar{\rho}$	$5242.7 \pm 2.6 \text{ kg m}^{-3}$

paper is arranged as follows: in Section 2 we describe the data and inversion methods; in Section 3 we present results and analysis, including parameter sensitivity analysis and inverted interior structure; in Section 4 we discuss the effects of different hypothetical MoI and different uncertainties of MoI and k_2 on the estimation of internal parameters; finally, we draw a conclusion in Section 5.

2 DATA AND INVERSION METHODS

2.1 Geodetic Data

In this study, we employed Venus’s mean radius R (Seidelmann et al. 2007), standard gravitational parameter GM (Konopliv et al. 1999), degree two tidal Love number k_2 with primary tidal flexing period 58.4 days (Konopliv & Yoder 1996) and normalized mean MoI I/MR^2 (Yoder 1995). These values are summarized in Table 1.

In Table 1, due to the lack of observation data on Venus surface and the extremely slow rotation of Venus, the mean MoI was not well determined (Kaula 1979). In previous studies, the mean MoI was widely considered to be around 0.33 (Yoder 1995; Zhang & Zhang 1995; Lodders et al. 1998; Mocquet et al. 2011). In our study, we choose a hypothetical value of 0.33 as the “observed” data of MoI and assume 5% of 0.33 as uncertainties (1σ), with further explanation on Appendix A. In addition, we also considered different hypothetical value of MoI and different uncertainties of MoI to study the effect of varied hypothetical MoI on inversion results, the results can be seen in the Supporting Information (<http://www.raa-journal.org/docs/Supp/ms4565SI.pdf>). The mean density and uncertainty was calculated from standard gravitational GM and Mean radius R with the gravitational constant $G = 6.674184(78) \times 10^{-11} \text{ m}^3 \text{ kg}^{-1} \text{ s}^{-2}$ (Li et al. 2018). The tidal Love number k_2 was estimated from Doppler tracking data of Pioneer Venus Orbiter (collected from December 1978 to September 1982) and the Magellan mission (collected from September 1992 to October 1994).

2.2 Inversion Method

To infer the internal structure model of Venus, we introduced a MCMC algorithm (Mosegaard & Tarantola 1995), an effective method to solve the nonlinear inverse problem. The posterior probability distributions of the models $\pi(\mathbf{m})$ are given as follows:

$$\pi(\mathbf{m}) = C \cdot \theta(\mathbf{m})L(\mathbf{m}), \quad (1)$$

where C is a constant coefficient; $\theta(\mathbf{m})$ is the a priori probability distribution of \mathbf{m} ; $L(\mathbf{m})$ is the likelihood function. We assume that the models of Venus is spherically symmetric and in hydrostatic equilibrium. To study the status of the Venus’s core, the models are divided into three and four isotropic layers respectively. The 3-layer model includes crust, mantle, and a liquid core. The 4-layer model includes crust, mantle, liquid outer core, and a solid inner core. The parameters of each layer of the models are the radius, mean density, viscosity, P-wave velocity (V_p), and S-wave velocity (V_s), which are based on the density and the Poisson ratio. The methodology is schematically illustrated in Figure 1.

As shown in Figure 1, the first step is to build an initial model. The parameters of the initial model are used to calculate the synthetic geodetic data ($\bar{\rho}$, MoI, and k_2). From this, the likelihood function $L(\mathbf{m})$, which measures the misfit between synthetic data and observed data, is obtained. We assume that the noise of the observations is Gaussian distributed and consider that observational uncertainties among the data sets to be independent. The $L(\mathbf{m})$ is given by

$$L(\mathbf{m}) \propto \exp \left\{ - \frac{[d_{\text{obs}}^{\text{MoI}} - d_{\text{cal}}^{\text{MoI}}(\mathbf{m})]^2}{2\sigma_{\text{MoI}}^2} - \frac{[d_{\text{obs}}^{k_2} - d_{\text{cal}}^{k_2}(\mathbf{m})]^2}{2\sigma_{k_2}^2} - \frac{[d_{\text{obs}}^{\bar{\rho}} - d_{\text{cal}}^{\bar{\rho}}(\mathbf{m})]^2}{2\sigma_{\bar{\rho}}^2} \right\}, \quad (2)$$

where d_{obs} , d_{cal} , σ are observed data, synthetically computed data of model, and the uncertainty on observed data, respectively. The tidal Love number k_2 and the normalized mean MoI are calculated using the approach outlined in Appendix B.

Second, these parameters are perturbed in a random walk way to build a new model \mathbf{m}_{i+1} . For the density and the core radius, the transition function between two steps is $\rho_{i+1} = \rho_i + N(0, \sigma^2)$, σ is adjusted to make the acceptance rate near 0.25 (Gelman et al. 1996); the transition probability of Poisson ratio is uniform. New synthetic values of each observed data and likelihood function $L(\mathbf{m}_{i+1})$ is obtained. Comparing the two-likelihood function, if $L(\mathbf{m}_{i+1})/L(\mathbf{m}_i) > 1$, a new model is accepted; if $L(\mathbf{m}_{i+1})/L(\mathbf{m}_i) \leq 1$, the new model is accepted

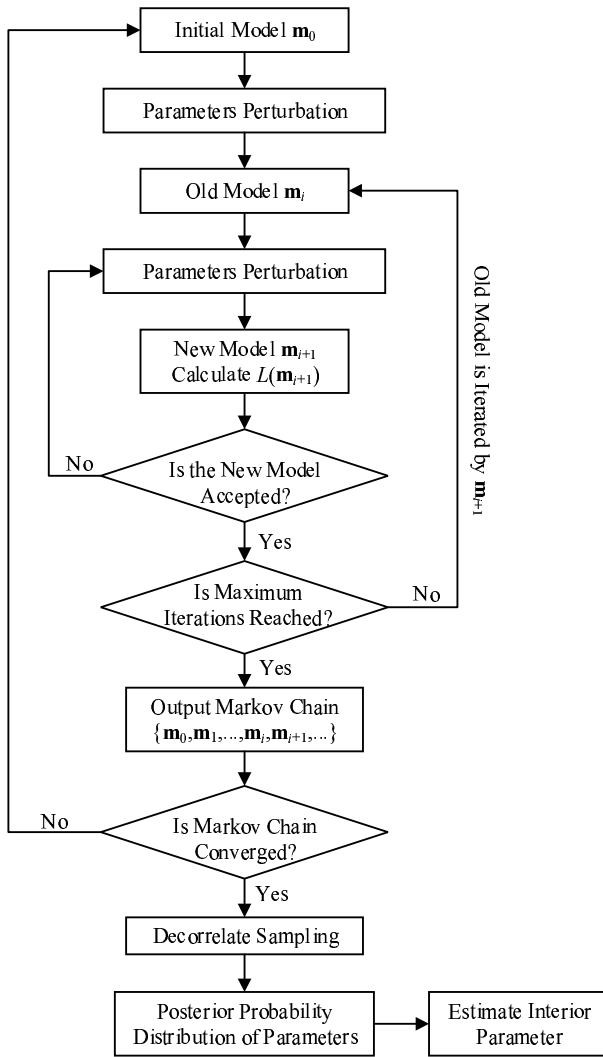


Fig. 1 Flow chart of the calculation process.

with probability $L(\mathbf{m}_{i+1})/L(\mathbf{m}_i)$, rejected with probability $1 - L(\mathbf{m}_{i+1})/L(\mathbf{m}_i)$. If the new model is rejected, then we do this step again to get an acceptable new model. The old model \mathbf{m}_i is replaced by the acceptable new model \mathbf{m}_{i+1} and does a new perturbation based on \mathbf{m}_{i+1} . Till the maximum number of iteration reached, all acceptable models are recorded to generate Markov Chains.

Third, we sample from the models of the Markov Chain, to reduce the effects of autocorrelation among them. The posterior probability distribution $\pi(\mathbf{m})$ can be obtained by these sampled models. Thus, the parameters of internal structure can be estimated from the posterior probability distributions and used to build the model of Venus.

3 RESULTS AND ANALYSIS

3.1 Parameters Sensitivity Analysis

Due to the limited quality of the currently geodetic data for Venus, some parameters that are not sensitive to the

geodetic data cannot be well constrained. Thus, we conducted a series of sensitivity studies on the parameters of each layer first. Detailed test results and analysis are given in Appendix C. In the previous studies, there are few differences in estimating the crustal thickness and density of Venus, based on different data and methods. However, the mass of Venus crust is only about 0.5% of the total mass of Venus; therefore small changes in the parameter of crust have little impact on final results of mean moment of inertia and tidal Love number k_2 . These parameters cannot be well constrained by current geodetic data. Thus, we set the parameters of crust as fixed values. Furthermore, to ensure parameter consistency, the model adopts Yoder's assumption for the Venus crustal structure (Yoder 1995). We set the crustal parameters as follows: the density of crust is 2850 kg m^{-3} , the viscosity of crust is 10^{22} Pa s , and Lamé coefficients are 56.4 and 35.8 GPa respectively.

In the mantle region, the sensitivity analysis indicates that the density and seismic velocity are sensitive to currently geodetic data. The core radius also has a significant impact on synthetic k_2 . However, the rheology model in our studies is adopted the Maxwell viscoelasticity, and tidal Love number k_2 does not change with a viscosity of mantle when the viscosity larger than 10^{18} Pa s . This means the mantle viscosity is not sensitive to k_2 under the current understanding of Venus. Therefore, we set the viscosity of mantle to 10^{21} Pa s (Parmentier & Hess 1992) and other parameters of mantle were regarded as free parameters.

The core region of the 3-layer and 4-layer models is discussed separately. The shear modulus of ideally liquid is considered to be zero, and we also assumed the viscosity of liquid core is 0 Pa s (de Wijs et al. 1998). The sensitive analysis of liquid core indicates that the P-wave velocity is not sensitive to tidal Love number k_2 . This is mainly due to our method, in Equations (B.9) and (B.10), y_5 and y_7 are not affected by λ . Therefore, only the density of liquid core is regarded as free parameters in the 3-layer model. In the 4-layer model, the liquid core part is similar to the 3-layer model, and the sensitivity analysis of solid inner core indicates that the density and radius of inner core are sensitive to the geodetic data. The sensitivity of viscosity relies on the radius of inner core. With a small inner core, viscosity is not sensitive to tidal Love number k_2 . However, it can be constrained if there is a large inner core within Venus (e.g., the radius of inner core is larger than 2500 km).

For a 3-layer model, the inverse problem is simplified by reducing the number of parameters needed to be inverted from 15 to 5. These five parameters are the mantle seismic velocity of P-wave and S-wave, the core radius, and the density of mantle and core. In addition, for a 4-layer model, the inverse problem is simplified by reducing the

number of parameters needed to be inverted from 20 to 8. These eight parameters are the mantle seismic velocity of P-wave and S-wave, the radius of the inner and outer core, the density of mantle, inner core and outer core, and the viscosity of inner core.

The a priori probabilities of parameters are based on the previous study (e.g., [Basaltic Volcanism Study Project 1981](#); [Lodders et al. 1998](#); [Steinberger et al. 2010](#); [Aitta 2012](#)). The a priori probability of mantle density is uniformly distributed between $3300\text{--}4600\text{ kg m}^{-3}$. The pressure in the center of Venus is about 275 GPa ([Steinberger et al. 2010](#)), which is less than the pressure at the center of the Earth. Thus the average density of Venus's core must be smaller than the density of Earth's core center (about 13000 kg m^{-3}). Based on the understanding of rocky type planets, the density increased by depth. Therefore, we added a restriction to the core density, which makes it less than 13000 kg m^{-3} and larger than the density of mantle, and the a priori probability distribution is uniform. For the 4-layer model, the density of the iron-rich solid core is uniformly distributed between $12000\text{--}13000\text{ kg m}^{-3}$, and the density of the liquid core is uniformly distributed between the solid core density and the mantle density. The viscosity of inner core is log-uniform distributed between $10^{14} - 10^{27}\text{ Pa s}$. The a priori probability of core radius is a uniform distribution. The a priori probability of Poisson ratio is uniformly distributed between $0.25\text{--}0.3$, which is a rough estimate from the PREM model ([Dziewonski & Anderson 1981](#)).

3.2 Inversion Results

We employed an MCMC algorithm in our inversion process for the 3-layer model with an entirely liquid core. In total, 10 Markov chains were generated, and length of each chain was one million. The first 30% of the chain was thrown away as a burn-in period ([Matsumoto et al. 2015](#)) and seven million models are collected. Then, we performed an autocorrelation analysis of each chain; the autocorrelation coefficient can be neglected after 850 orders. In that case, we sampled 8240 models from these seven million models, which reduce the autocorrelation of models. The posterior probability distribution of the obtained models and parameters is shown in Figure 2.

Figures 2(a), (b) and (c) show the joint probability density functions of each pair of synthetic geodetic data. These functions were generated by the covariance matrices of each pair MoI, k_2 , and mean density and their expectations, rather than the spread of results data point. The correlation coefficient of MoI and k_2 is -0.357 ; the correlation coefficient of MoI and mean density is 4.840×10^{-3} ; the correlation coefficient of k_2 and mean density is -3.805×10^{-4} .

Figures 2(d), (e) and (f) show that the posterior probability distributions of mean moment of inertia, tidal Love number k_2 and mean density are similar to the geodetic data. This indicates that the sampled models fit the geodetic data well. Figure 2(g) shows the posterior probability distribution of mantle density with the optimal value of 4101 kg m^{-3} , which is at the highest frequency. Based on the normal distribution hypothesis, the mantle density is estimated as $4076 \pm 350\text{ kg m}^{-3}$ (1σ). Figure 2(h) shows the posterior probability distribution of the core radius and the optimal value is 3294 km . The core radius, based on a normal distribution hypothesis, is estimated as $3271 \pm 238\text{ km}$ (1σ). Figure 2(i) shows the posterior probability distribution of core density. The optimal value of core density is 11885 kg m^{-3} . However, the normal distribution hypothesis is rejected by the distribution of core density. Figure 2(j) shows the posterior probability distribution of S-wave velocity in mantle with the optimal value of 6720 m s^{-1} , which is at the highest frequency. Based on the normal distribution hypothesis, the mantle S-wave velocity is estimated as $6690 \pm 701\text{ m s}^{-1}$ (1σ). Figure 2(k) shows the posterior probability distribution of P-wave velocity in mantle with the optimal value of 9707 m s^{-1} , which is at the highest frequency. Based on the normal distribution hypothesis, the mantle P-wave velocity is estimated as $9833 \pm 776\text{ m s}^{-1}$ (1σ).

As shown in the sensitivity analysis in Appendix C, there are many trade-offs between pairs of interior parameters. We also give the joint probability density function of pairs of interior parameters, which is shown in Figure 3. Since the models should match the observations of mass and radius, the core density and mantle density have a negative correlation, as shown in Figure 3(a). For the same reason, the density of mantle and the core radius have a strong negative correlation, as shown in Figure 3(b). The calculation of k_2 is closely related to the shear modulus of the mantle ($\mu = \rho V_s^2$), thus there are negative correlation between mantle density and S-wave velocity, and positive correlation between core radius and S-wave velocity, as shown in Figures 3(c) and (h). Other pairs of interior parameters seem to be weakly correlated or unrelated (correlated coefficient less than 0.3).

Another issue is that it was hard to give the tolerance scope of core density based on one-dimensional posterior probability distribution. To address this issue, we constrained core density by using core radius as an auxiliary condition. This condition was given by one-dimensional posterior probability distribution. For a one-dimensional Gaussian distribution, there are about 68% of the models within $\pm 1\sigma$. To determine the tolerance scope of core density, we want to find an area contains 68% of the models whose core radius range from 3033 to 3509 kg m^{-3} ,

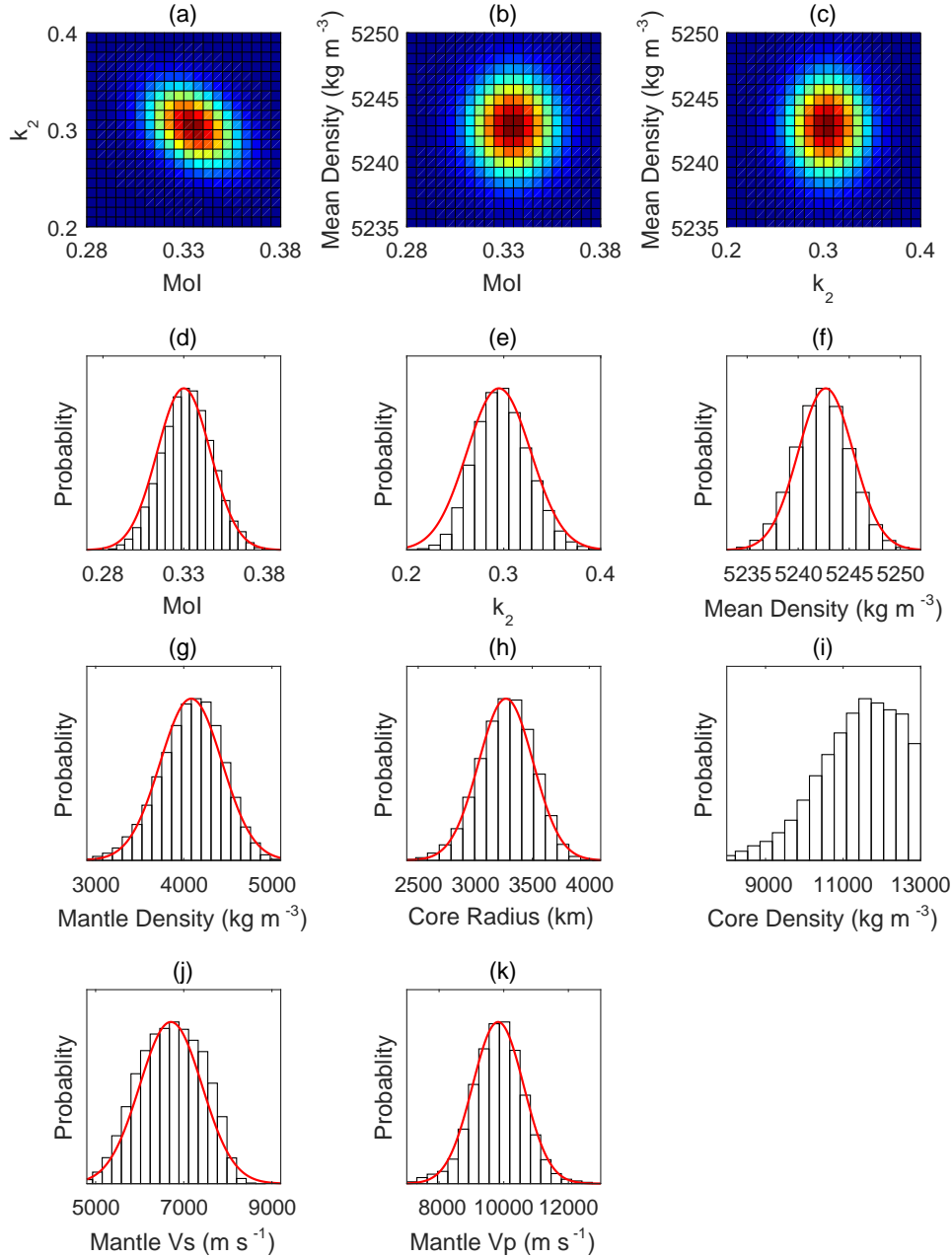


Fig. 2 The joint probability density function between (a) mean moment of inertia and k_2 ; (b) mean density and mean moment of inertia; (c) mean density and k_2 ; The posterior probability distribution of the synthetic geodetic data and parameters (d) mean moment of inertia; (e) tidal Love number k_2 ; (f) mean density; (g) density of mantle; (h) core radius (CMB); (i) density of liquid core; (j) S-wave velocity of mantle; (k) P-wave velocity of the mantle. The *red curves* in (d) (e) and (f) indicate the geodetic data and *red curves* in (g) (h) (j) and (k) are the normal distribution curves based on results.

and make this area as small as possible. As shown in Figure 4, under the constraint of core radius, there are 68% models located in the area with core density ranging from 10643 to 12840 kg m^{-3} . By combining with the optimal value of core density, the core density is estimated as 11885^{+955}_{-1242} kg m^{-3} .

Considering that the mean MoI of Venus cannot be obtained by current observations and the parameter estimations are strongly affected by the hypothetical value of MoI, we also performed inversion on different values of MoI to study its influence on the parameters estimation. We choose 0.34 which is close to the upper limit of the estimated Venus MoI (i.e., 0.341, Dumoulin et al. 2017) and

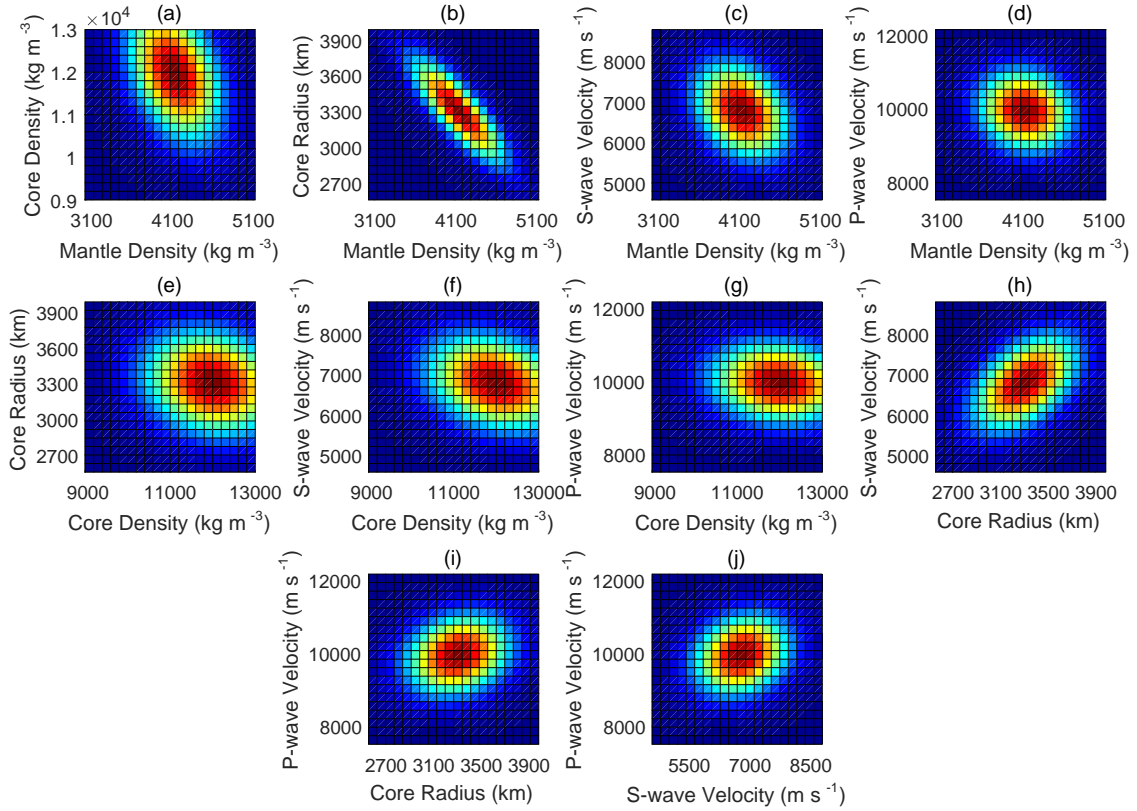


Fig. 3 The joint probability density function of each pairs of interior parameters. (a) mantle density and core density; (b) mantle density and core radius; (c) mantle density and S-wave velocity; (d) mantle density and P-wave velocity; (e) core density and core radius; (f) core density and S-wave velocity; (g) core density and P-wave velocity; (h) core radius and S-wave velocity; (i) core radius and P-wave velocity; (j) S-wave velocity and P-wave velocity.

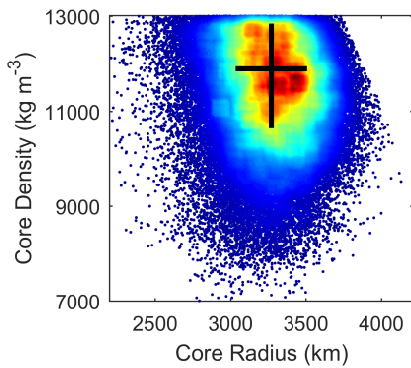


Fig. 4 Two-dimensional posterior probability distributions of core density and core radius, color indicate the possibility: *red* means high probability density and the *blue* means low probability density; the tolerance scopes with 1σ are present by *black line*.

0.32 which is much low than current MoI estimations. The results are shown in the Supporting Information (Figs. S1 and S2).

With the hypothetical MoI increase, the density of mantle increased and the core radius decreased. To ensure

the total mass and radius consistent with the observations, the core density also increased with the MoI. In addition, the seismic velocity will also decrease as the mantle density increases to ensure the Lamé coefficient (λ and μ) of the mantle matches the observation of k_2 .

We also generated 10 Markov Chains for the 4-layer model which contain both solid inner core and liquid outer core, each chain with a length of one million. We throw away 30% of the chain and sampled from the remaining chain to reduce the autocorrelation, as we did in 3-layer model. The posterior probability distribution of the obtained models is shown in Figure 5.

In Figures 5(a), (b) and (c), the joint probability density functions of each pair of synthetic geodetic data are shown. The correlation coefficient of MoI and k_2 is -0.426 ; the correlation coefficient of MoI and mean density is 4.936×10^{-3} ; the correlation coefficient of k_2 and mean density is 6.987×10^{-3} . Figure 5(f) shows that the posterior probability distribution of mean density is similar to the observation, however, the posterior probability distributions of mean moment of inertia and tidal Love number k_2 are slightly biased from the observations with-

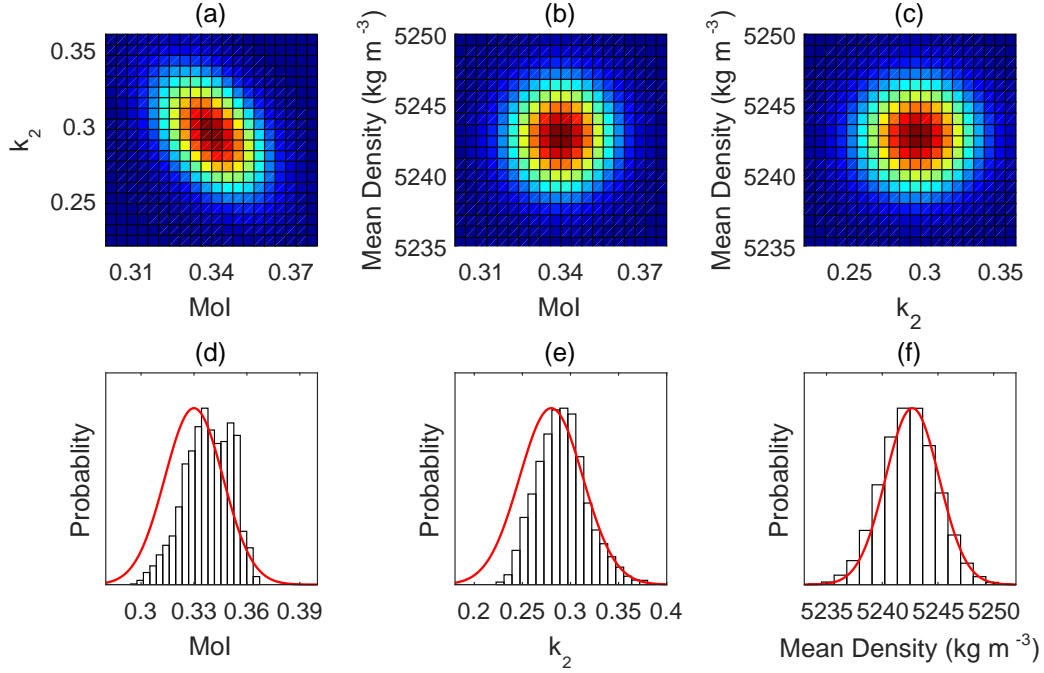


Fig. 5 The joint probability density function between (a) mean moment of inertia and k_2 ; (b) mean density and mean moment of inertia; (c) mean density and k_2 ; The posterior probability distribution of the synthetic geodetic data (d) mean moment of inertia; (e) tidal Love number k_2 ; (f) mean density. The red curves in (d), (e) and (f) indicate the geodetic data.

in 1σ . The synthetic data of MoI is slightly larger than the geodetic data and the value of k_2 is slightly smaller than the observed data. Furthermore, both the posterior probability distribution of MoI and k_2 reject the normal distribution hypothesis.

4 DISCUSSION

By comparing the results of 3-layer model and 4-layer model, we found that the 3-layer model, which only contain an entire liquid core, can better satisfy the geodetic data. However, due to the limited quality of the observed data, the posterior probability distribution of k_2 did not exceed the range of currently observed data. Thus, we could not completely reject the hypothesis of the existence of solid inner core. If the uncertainties of the observed k_2 (and also the MoI) are greatly reduced in future, like the accuracy of those of Mars (Konopliv et al. 2016) and the Moon (Williams & Boggs 2015), the core state of Venus will be better understood.

Based on the assumption of 3-layer model, our inversion results of the mantle and core density of Venus are 4101_{-375}^{+325} and 11885_{-1242}^{+955} kg m⁻³, respectively. Our results are close to the research of Lodders et al. (1998), who found an average density of the mantle and core of Venus are 4000 and 12000 kg m⁻³ respectively by using a 3-layer model. However, our results are different from Aitta (2012)’s study, which assumed that the density varies

with depth. In the results of Aitta, the average densities of core and mantle are 4600 and 10600 kg m⁻³, respectively. For Aitta’s 1 km-layer model, the calculated MoI is 0.338; based on the assumption of isotropic 3-layer model with the mean density given by Aitta, the value of calculated MoI will be 0.347. On the one hand, the geodetic data of MoI we used (0.33 ± 0.0165) is slightly different from Aitta. On the other hand, even if the observed data are the same, the different assumption of model structure will cause the different solution of interior parameters.

Our results imply that the core radius of Venus is 3294_{-261}^{+215} km, and is larger than the value estimated in previous research. The value of tidal Love number k_2 used in previous research is less than 0.29 (e.g., Yoder 1995; Xia & Xiao 2002; Zhang & Zhang 1995). However, our research uses Konopliv & Yoder (1996)’s observed data which is 0.295 ± 0.066 and contain the value larger than 0.29. As shown in Figure C.1, the tidal Love number k_2 was positively correlated with core radius. Therefore, we argue that Venus has a larger liquid core than in previous studies.

We performed a numerical simulation to test the effect of more accurate MoI and Love number k_2 on the interior parameter estimations. We assume a “True Model” with $\rho_{\text{mantle}} = 4000$ kg m⁻³, $\rho_{\text{core}} = 12493$ kg m⁻³, $r_{\text{core}} = 3200$ km, $V_s = 6400$ m s⁻¹, and $V_p = 9500$ m s⁻¹. Thus the synthetic value of k_2 , MoI and mean density of

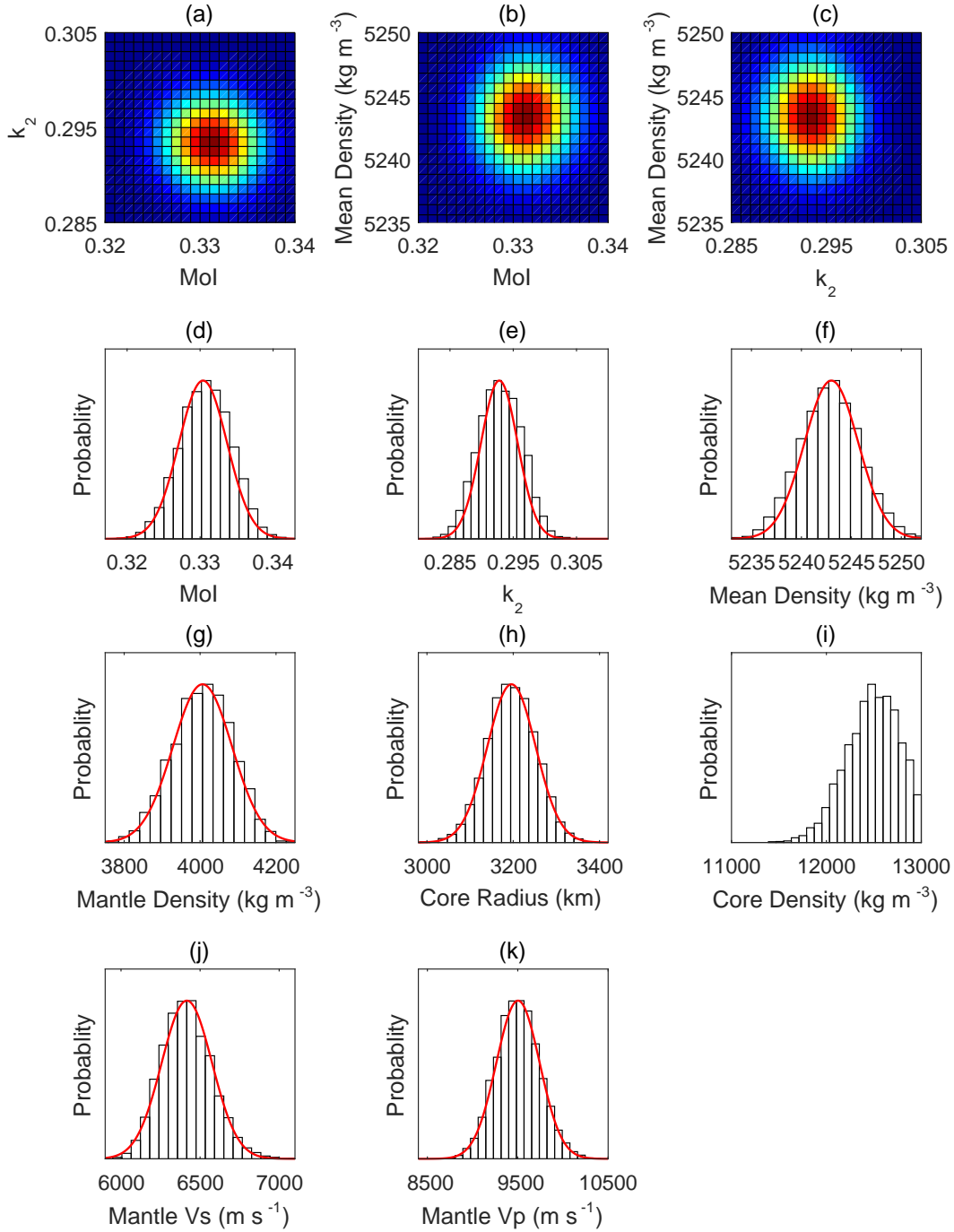


Fig. 6 The joint probability density function between (a) mean moment of inertia and k_2 ; (b) mean density and mean moment of inertia; (c) mean density and k_2 . The posterior probability distribution results of numerical simulation-1. (d) mean moment of inertia; (e) tidal Love number k_2 ; (f) mean density; (g) density of mantle; (h) core radius (CMB); (i) density of liquid core; (j) S-wave velocity of mantle; (k) P-wave velocity of the mantle. The *red curves* in (d), (e) and (f) indicate the assumed geodetic data and *red curves* in (g) to (k) are normal distribution curves based on results.

the True Model are 0.2928, 0.3304 and 5243 kg m^{-3} , respectively. We keep the uncertainties of mean density as $\pm 2.6 \text{ kg m}^{-3}$ which is consistent with the geodetic data listed in Table 1. We add a 1% noise of k_2 and MoI, respectively. The inversion results are shown in Figure 6. In addition,

we also studied the effect of different level of noise on parameter estimations, the results are listed in Table 2 and the posterior probability distributions shown in Supporting Information (Figs. S3–S6).

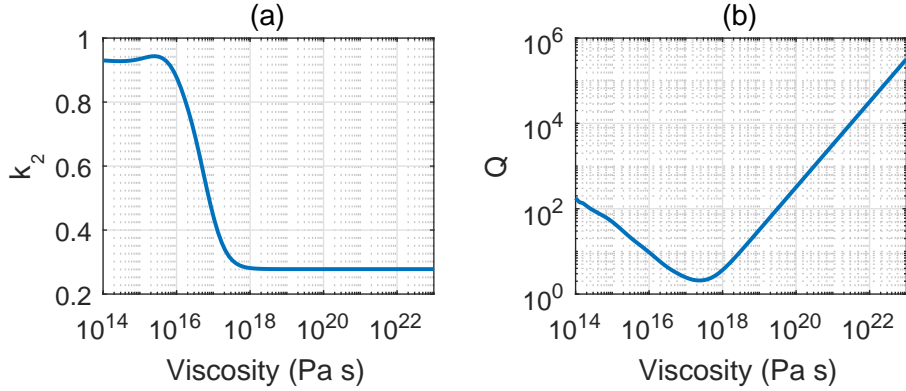


Fig. 7 (a) The response of tidal Love number k_2 to varying viscosity of mantle; (b) The response of dissipation factor Q to varying viscosity of mantle.

Table 2 Inversion Results of Numerical Simulations

No.	k_2	MoI	ρ_{mantle} [kg m^{-3}]	r_{core} [km]	ρ_{core} [kg m^{-3}]	V_s [m s^{-1}]	V_p [m s^{-1}]	Figure
1	0.2928 ± 0.0029	0.3304 ± 0.0033	4006 ± 78	3196 ± 56	12480 ± 274	6416 ± 159	9503 ± 239	Figure 6
2	0.2928 ± 0.0029	0.3304 ± 0.0100	4071 ± 168	3171 ± 89	12490 ± 490	6417 ± 168	9513 ± 249	Figure S3
3	0.2928 ± 0.0100	0.3304 ± 0.0100	4089 ± 197	3173 ± 126	12450^{+550}_{-573}	6453 ± 279	9557 ± 416	Figure S4
4	0.2928 ± 0.0100	0.3304 ± 0.0165	4160 ± 279	3152 ± 161	12510^{+490}_{-935}	6527 ± 324	9565 ± 440	Figure S5
5	0.2928 ± 0.0330	0.3304 ± 0.0165	4127 ± 349	3192 ± 268	12433^{+567}_{-1018}	6590 ± 697	9724 ± 802	Figure S6

As shown in Figures 6(g)–(j), the mantle density is $4006 \pm 78 \text{ kg m}^{-3}$; the core radius is $3196 \pm 56 \text{ km}$; the core density is $12480 \pm 274 \text{ kg m}^{-3}$; the S-wave velocity is $6416 \pm 159 \text{ m s}^{-1}$; the P-wave velocity is $9503 \pm 239 \text{ m s}^{-1}$. Comparing the results with Simulation-5, which has the same level noise of the geodetic data listed in Table 1, we found that the uncertainty of interior parameters reduced significantly. In addition, the expectation of the posterior probability distribution is almost the same as the “True Model”. Moreover, we found the mantle density and core radius decreases significantly with the decreased noise of MoI, while the seismic wave velocities are strongly related to the noise level of k_2 . Therefore, values with higher accuracy for k_2 and MoI are needed to constrain further the interior parameters; however, given our 3-layer model assumption, the inverted P-wave and S-wave velocity of the mantle reflect the average velocity of seismic wave rather than the seismic velocity profile, which varies with depth. To obtain this seismic velocity profile, an array of seismic stations on the surface of Venus is required.

The viscosity is one of the key parameters to build Venus internal structure and used to calculate tidal Love number k_2 . Unfortunately, the viscosity cannot be well constrained by the currently available geodetic data. The crustal viscosity can be obtained by combining the mineral composition obtained from surface sampling in the future and rheological results from laboratory rock experiment (Bürgmann & Dresen 2008). However, the viscosity

of mantle and core cannot be obtained directly. In this case, we want to find out whether other geodetic data can be used to constrain viscosity. Furthermore, we found that the tidal dissipation factor Q is sensitive to the mantle viscosity. The sensitivity analysis of the viscosity of mantle and the tidal dissipation factor Q is shown in Figure 7.

As shown in Figure 7, the synthetic values of tidal dissipation factor Q calculated by forward modeling method range from 2 to 5×10^5 when the viscosity of mantle varies from 10^{14} to 10^{23} Pa s . In addition, the tidal dissipation factor Q is sensitive to mantle viscosity larger than 10^{18} Pa s , which the tidal Love number k_2 is not sensitive. Therefore, if there is observed data of Q in the future, then the viscosity of Venus mantle can be constrained well.

5 CONCLUSIONS

We used the MCMC algorithm to obtain the parameters of 3-layer and 4-layer isotropic spherical symmetric model of Venus as constrained by current geodetic data and prior information. The 3-layer model fits the geodetic data; however, the 4-layer model is slightly biased by the geodetic data. Thus, based on our results, a liquid core inside Venus is more credible than a solid inner core with a liquid outer core. However, the complete negation of the solid inner core thesis requires data that are more accurate. In consideration of available geodetic data, we estimated the interior parameters of Venus based on the assumption of 3-layer model.

Based on the sensitivity analysis of 3-layer model, the goal of this paper is to invert the average density of the mantle and core, the seismic wave velocity of the mantle, and the core radius of Venus by using current geodetic data. The following conclusions are drawn: based on currently geodetic data ($k_2 = 0.295 \pm 0.066$, $I/MR^2 = 0.33 \pm 0.0165$, and $\bar{\rho} = 5242 \pm 2.6 \text{ kg m}^{-3}$), the core radius of Venus is 3294_{-261}^{+215} km, the average mantle density of Venus is 4101_{-375}^{+325} kg m^{-3} , the average density of the liquid core of Venus is 11885_{-1242}^{+955} kg m^{-3} , and the P-wave and S-wave velocities of the mantle of Venus are 9707_{-650}^{+902} and 6720_{-731}^{+671} m s^{-1} , respectively. Our results indicate that there is a larger core in Venus. Considering that Venus's MoI cannot be obtained by any direct observations at present, we also provide the other inverted results based on different hypothetical value of MoI. It suggested that the internal structure of Venus cannot be uniquely determined by current tidal Love number k_2 solely.

Considering of future Venus missions and the possibility to improve the accuracy of observations, we simulated a numerical calculation with the assumption of different uncertainties in the k_2 and MoI to study the influence of the improved accuracy on inversion results. We found that about 1% uncertainty of the geodetic data was sufficient to estimate the interior parameters.

Due to the limited quality of the observed data, the viscosity of mantle cannot be only constrained by current tidal Love number k_2 . However, the viscosity of the mantle is sensitive to the tidal dissipation factor Q, and this result is consistent with other published research (Dumoulin et al. 2017). Thus, if the tidal dissipation factor Q of Venus can be obtained, then it will boost internal structure research.

In future work, our understanding of Venus interior can be improved in terms of data and model assumptions. Directly measured seismic data would boost our understanding of the internal structure of Venus. A workshop on the feasibility and technical details of building a seismic station on the surface of Venus (Stevenson et al. 2015) was organized by the Keck Institute for Space Studies (KISS) in 2015. If we consider an inversion model that assumes that density and seismic velocity vary with depth, then the results will be closer to the real situation. Simultaneously, higher accuracy orbital tracking and lander data will improve the constraint of the seismic velocity profile.

Acknowledgements We thank an anonymous reviewer for a careful review and constructive comments. This work is supported by the National Natural Science Foundation of China (U1831132, 41874010), Innovation Group of Natural Fund of Hubei Province (2018CFA087), the Science and Technology Development Fund of Macau Special Administrative Region (FDCT 007/2016/A1, 119/2017/A3, 187/2017/A3), and Guizhou Provincial Key

Laboratory of Radio Astronomy and Data Processing (KF201813).

Appendix A: ANALYSIS OF MOI

The mean MoI of Venus was not well determined, especially because of the slow spin rate of Venus (Kaula 1979; Mocquet et al. 2011). However, without the constraint of mean MoI, the synthetic MoI of models tended to approach 0.4 (See Fig. A.1). It indicated that the model of Venus likely to be a uniform sphere, which is far from the results of previous studies. We performed the additional simulate inversion without the MoI, and the result is shown in Figure A.1.

As shown in Figure A.1(a), the mean MoI of models tends to be closer to 0.4. Besides, Figure A.1(b) and (c) show that the posterior probability distribution of k_2 and mean density fit the observations well. As shown in Figure A.1(d), the mantle density tends to approach the mean density, with the value of 5242 kg m^{-3} . The estimate of core radius is 2986_{-485}^{+371} km, as shown in Figure A.1(e), which is less than our results in Section 3. From Figure A.1(f), we see the core density is almost randomly distributed within the search space. The results indicate that, without the constraint of MoI, the model would become unrealistic and unsuitable for estimating some of the parameters. However, if we use MoI as a condition to sample from the simulation results, we are able to estimate the parameters. The results of sampled models are shown in Figure A.2.

Compared with the results of our inversion in Section 3, the probability distributions obtained by these two methods are almost the same. That is to say, our solution is included in the inversion results without the constraint of MoI. Therefore, we considered the MoI as constraints and used a widely recognized MoI value of 0.33 (Yoder 1995; Zhang & Zhang 1995; Dumoulin et al. 2017).

Appendix B: EQUATIONS

Our model is in hydrostatic equilibrium and divided into three or four spherically symmetric layers. The total mass and mean moment of inertia of three layer model are computed as:

$$M = \frac{4}{3}\pi [\rho_{\text{lc}}r_{\text{lc}}^3 + \rho_{\text{mantle}}(r_{\text{mantle}}^3 - r_{\text{lc}}^3) + \rho_{\text{crust}}(r_{\text{crust}}^3 - r_{\text{mantle}}^3)], \quad (\text{B.1})$$

$$\frac{I}{MR^2} = \frac{2}{5} \left[\frac{\rho_{\text{crust}}}{\bar{\rho}} + \frac{\rho_{\text{mantle}} - \rho_{\text{crust}}}{\bar{\rho}} \left(\frac{r_{\text{mantle}}}{R} \right)^5 + \frac{\rho_{\text{lc}} - \rho_{\text{mantle}}}{\bar{\rho}} \left(\frac{r_{\text{lc}}}{R} \right)^5 \right], \quad (\text{B.2})$$

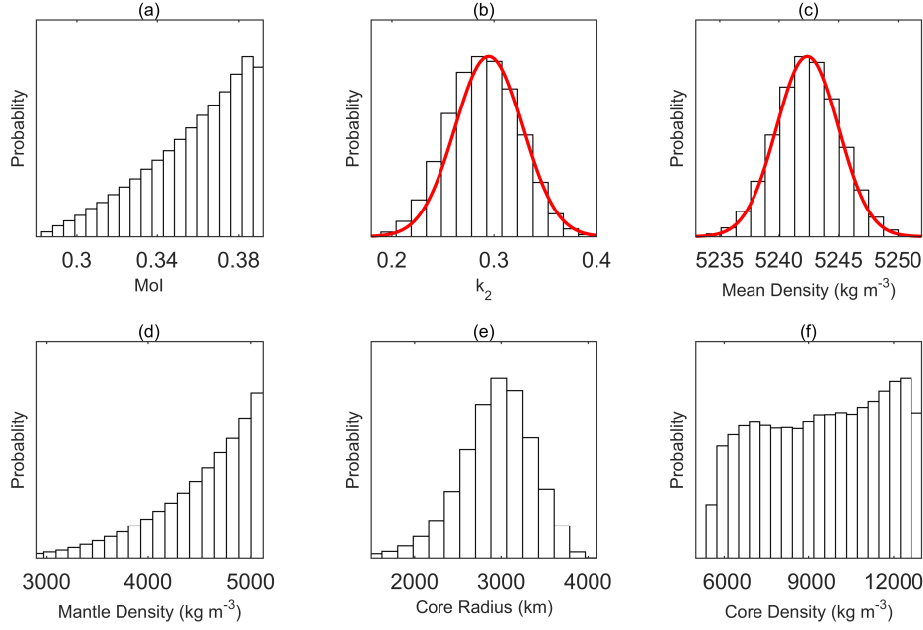


Fig. A.1 Posterior probability distribution. (a) mean moment of inertia; (b) tidal Love number k_2 ; (c) mean density; (d) density of mantle; (e) core radius (CMB); (f) density of liquid core; the *red line* in (b) and (c) indicates the observed data of k_2 and mean density.

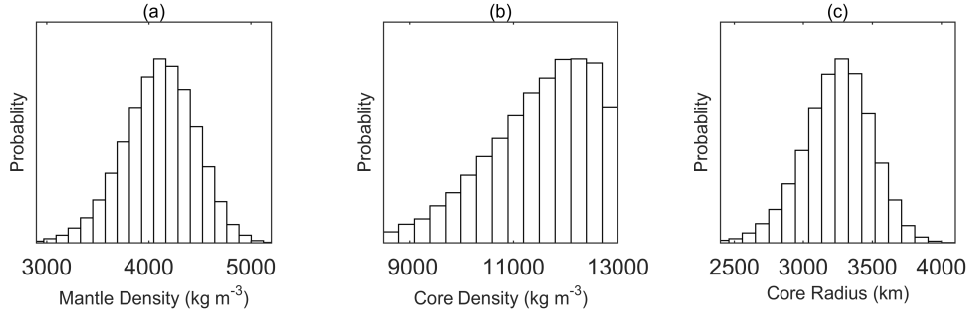


Fig. A.2 Posterior probability distribution of sampled models (a) density of mantle; (b) density of liquid core; (c) core radius (CMB).

where ρ_{crust} , ρ_{mantle} , and ρ_{lc} are the density of Venusian crust, mantle, and liquid core, respectively; $\bar{\rho}$ is the mean density of Venus, R is the radius of Venus, and r_{mantle} , r_{lc} are the radius of mantle (Moho surface) and core (CMB), respectively. The four layer model is similar to Equations (B.1) and (B.2), that a term of solid core is added.

To solve the tidal Love number k_2 , we basically follow the formulation proposed by Takeuchi & Saito (1972), which originated from Alterman et al. (1959). In addition, the calculation for a liquid part is simplified based on the formulation of Saito (1974), the differential formulations for solid layer are written as:

$$\frac{dy_1}{dr} = \frac{1}{\lambda + 2\mu} \left\{ y_2 - \frac{\lambda}{r} [2y_1 - n(n+1)y_3] \right\}, \quad (\text{B.3})$$

$$\begin{aligned} \frac{dy_2}{dr} &= \frac{2}{r} \left(\lambda \frac{dy_1}{dr} - y_2 \right) \\ &+ \frac{1}{r} \left(\frac{2(\lambda + \mu)}{r} - \rho g \right) [2y_1 - n(n+1)y_3] \\ &+ \frac{n(n+1)}{r} y_4 - \rho \left(y_6 - \frac{n+1}{r} y_5 + \frac{2g}{r} y_1 \right), \end{aligned} \quad (\text{B.4})$$

$$\frac{dy_3}{dr} = \frac{1}{\mu} y_4 + \frac{1}{r} (y_3 - y_1), \quad (\text{B.5})$$

$$\begin{aligned} \frac{dy_4}{dr} &= -\frac{\lambda}{r} \frac{dy_1}{dr} - \frac{\lambda + 2\mu}{r^2} [2y_1 - n(n+1)y_3] \\ &+ \frac{2\mu}{r^2} (y_1 - y_3) - \frac{3}{r} y_4 - \frac{\rho}{r} (y_5 - g y_1), \end{aligned} \quad (\text{B.6})$$

$$\frac{dy_5}{dr} = y_6 + 4\pi G \rho y_1 - \frac{n+1}{r} y_5, \quad (\text{B.7})$$

$$\frac{dy_6}{dr} = \frac{n-1}{r}(y_6 + 4\pi G\rho y_1) + \frac{4\pi G\rho}{r}[2y_1 - n(n+1)y_3]. \quad (\text{B.8})$$

The liquid layer is written as:

$$\frac{dy_5}{dr} = \left(\frac{4\pi G\rho}{g} - \frac{n+1}{r} \right) y_5 + y_7, \quad (\text{B.9})$$

$$\frac{dy_7}{dr} = \frac{2(n-1)}{r} \frac{4\pi G\rho}{g} y_5 + \left(\frac{n-1}{r} - \frac{4\pi G\rho}{g} \right) y_7. \quad (\text{B.10})$$

Here we consider Maxwell viscoelasticity as the rheological law for tidal deformation (e.g., [Peltier 1974](#)). The complex elastic moduli are derived as:

$$\tilde{\mu} = \frac{i\omega\mu}{i\omega + \frac{\mu}{\nu}}, \quad (\text{B.11})$$

$$\tilde{\lambda} = \frac{i\omega\lambda + \frac{\kappa\mu}{\nu}}{i\omega + \frac{\mu}{\nu}}, \quad (\text{B.12})$$

where ν is viscosity and the real moduli are:

$$\mu = \rho V_s^2, \quad (\text{B.13})$$

$$\lambda = \rho V_p^2 - 2\mu. \quad (\text{B.14})$$

Bulk modulus κ is

$$\kappa = \lambda + \frac{2}{3}\mu. \quad (\text{B.15})$$

Tidal frequency ω is written as:

$$\omega = \frac{2\pi}{T}. \quad (\text{B.16})$$

T is solid tidal period and i in Equations (B.11) and (B.12) is an imaginary unit.

By using Equations (B.3) to (B.10), y_1 to y_7 are calculated from core to surface layer by layer. Finally, on the surface, tidal Love numbers can be obtained:

$$h_2 = gy_1, \quad (\text{B.17})$$

$$l_2 = gy_3, \quad (\text{B.18})$$

$$k_2 = y_5 - 1. \quad (\text{B.19})$$

With the complex moduli, tidal Love number k_2 is a complex number, but its modulus is needed in the final calculation, expressed as:

$$|k_2| = \sqrt{[\Re(k_2)]^2 + [\Im(k_2)]^2}. \quad (\text{B.20})$$

Tidal dissipation factor Q is calculated as follows:

$$Q = \frac{|k_2|}{\Im(k_2)}. \quad (\text{B.21})$$

Because the formulation is singular at the center of the model, we set a 1 km radius uniform sphere in the center of model as the initial condition.

Appendix C: SENSITIVITY ANALYSIS

This section is focused on the response of tidal Love number k_2 , the mean MoI and the mean density to the changes in the interior parameters of each layer. Whether the synthetic data obtained from the models are consistent with observed data is not the primary concern in this section. We set an initial model, in which the radius, average density, viscosity, and seismic velocity of each layer are fixed values. One or two parameters were changed and used to calculate a series of forward models to determine the sensitivity of tidal Love number k_2 , the mean MoI and the mean density to changes in the interior parameters.

From Equations (B.1) and (B.2), the mean density and mean MoI are calculated directly using the density and thickness of each layer, as the mean density and mean MoI are sensitive to interior parameters. However, the uncertainty in the MoI is large for crustal parameters. In previous studies, the crustal thickness ranged from 10 to 30 km, crustal density ranged from 2800 to 2900 kg m⁻³, and the synthetic MoI data had less than 0.5% difference. For synthetic k_2 data, the difference was about 0.3%. Considering the quality of current observations, we set the parameters of the crust as fixed values.

Mean density is calculated by the density and thickness of each layer, as the quality of observed mean density data is accurate enough to constrain the mantle density and thickness. We analyzed the sensitivity of mantle parameters to the tidal Love number k_2 and mean moment of inertia, the results are shown in Figure C.1.

From Figure C.1(a) we found that when core radius varies from 3100 to 3300 km and the density of mantle varies from 3700 to 4200 kg m⁻³, the synthetic k_2 calculated by forward model ranges from 0.244 to 0.307. From Figure C.1(b) we found when core radius varies from 3100 to 3300 km and S-wave velocity of mantle varies from 6500 to 7500 m s⁻¹, the synthetic k_2 calculated by forward model ranges from 0.248 to 0.310. From Figures C.1(c) we found when core radius varies from 3100 to 3300 km and P-wave velocity of mantle varies from 9000 to 11000 m s⁻¹, the synthetic k_2 calculated by forward model ranges from 0.261 to 0.318. In addition, in Figure C.1(d) we found that when core radius varies from 3100 to 3300 km and viscosity of mantle varies from 10¹⁴ to 10²³ Pa s, the synthetic tidal Love number k_2 changed in a very large range. However when viscosity of mantle is larger than 10¹⁸ Pa s, which is similar to Earth mantle, k_2 has almost no change. From Figure C.1(e) we found that when core radius varies from 3100 to 3300 km and density of mantle varies from 3700 to 4200 kg m⁻³, the synthetic MoI calculated by forward model ranges from 0.312 to 0.342. Then we analyzed the sensitivity of core parameters

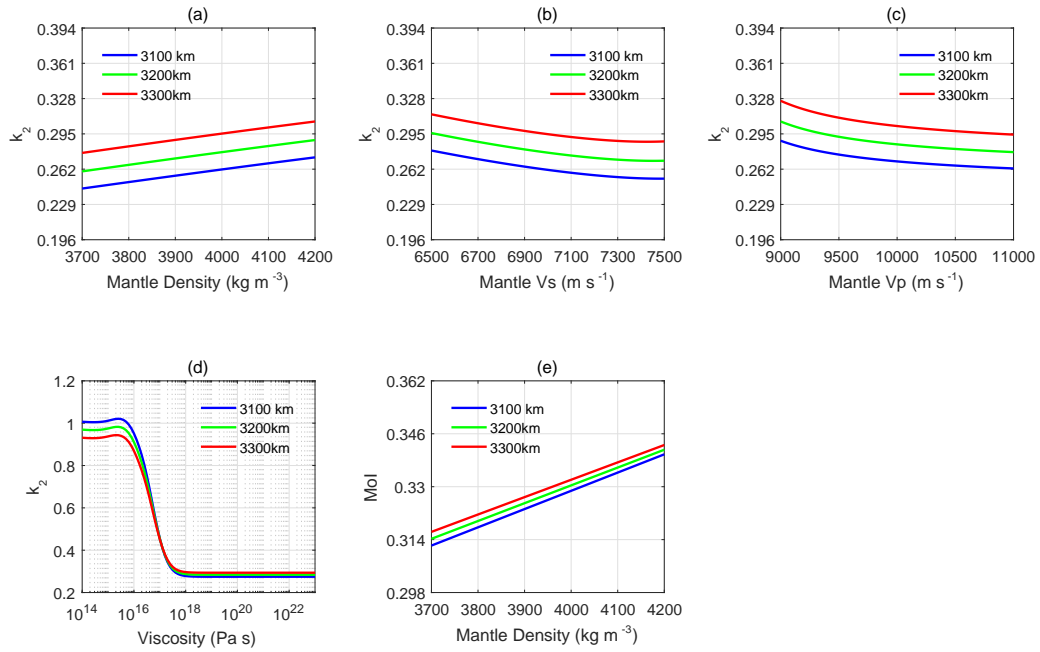


Fig. C.1 Sensitive analysis of mantle parameters, different colors represent core radius (CMB): *blue curve* is 3100 km, *green curve* is 3200 km and *red curve* is 3300 km. (a) Density of mantle and k_2 ; (b) S-wave velocity of mantle and k_2 ; (c) P-wave velocity of mantle and k_2 ; (d) viscosity of mantle and k_2 ; (e) density of mantle and Mol.

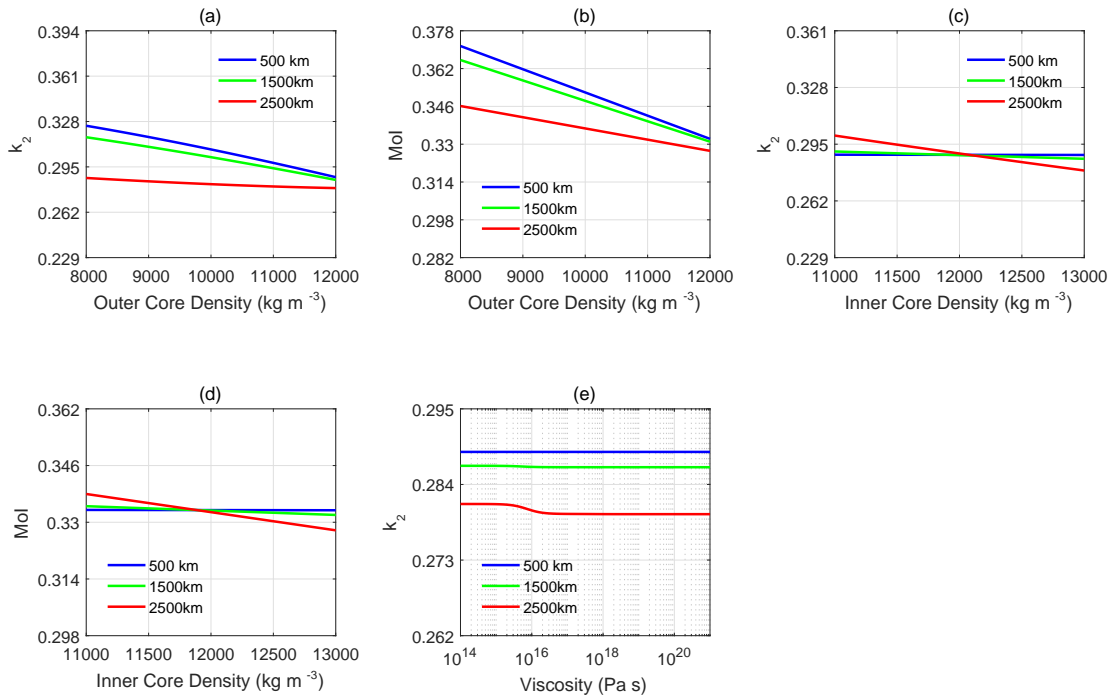


Fig. C.2 Sensitive analysis of core parameters, different colors represent inner core radius: *blue curve* is 500 km, *green curve* is 1500 km and *red curve* is 2500 km. (a) Density of outer core and k_2 ; (b) density of outer core and Mol; (c) density of inner core and k_2 ; (d) density of inner core and Mol; (e) viscosity of inner core and k_2 .

to tidal Love number k_2 and mean moment of inertia. The results are shown in Figure C.2.

From Figures C.2(a) and (b), we found that when the inner core radius varies from 500 to 2500 km and the density of the core varies from 8000 to 12000 kg m⁻³, the synthetic data of k_2 calculated by forward model ranges from 0.281 to 0.328 and the value of MoI ranges from 0.326 to 0.371. From Figures C.2(c) and (d), we found that when the inner core radius varies from 500 to 2500 km and the density of the inner core varies from 11000 to 13000 kg m⁻³, the synthetic data of k_2 calculated by forward model ranges from 0.282 to 0.302 and the value of MoI ranges from 0.325 to 0.337. We investigated a large range of viscosity from 10¹⁴ to 10²¹ Pa s, which is shown in Figure C.2(e). From Figure C.2(e), we found that if the inner core radius is 2500 km, k_2 changes with a viscosity of inner core; however, if the inner core radius is less than 1500 km, k_2 is insensitive to the viscosity of the inner core.

References

- Aitta, A. 2010, *Physics of the Earth and Planetary Interiors*, 181, 132
- Aitta, A. 2012, *Icarus*, 218, 967
- Alterman, Z., Jarosch, H., & Pekeris, C. L. 1959, in *Proceedings of the Royal Society of London Series A*, 252, 80
- Basaltic Volcanism Study Project. 1981, *Basaltic Volcanism on the Terrestrial Planets* (New York: Pergamon Press)
- Bills, B. G., Currey, D. R., & Marshall, G. A. 1994, *J. Geophys. Res.*, 99, 22,059
- Buck, W. R. 1992, *Geophys. Res. Lett.*, 19, 2111
- Bürgmann, R., & Dresen, G. 2008, *Annual Review of Earth and Planetary Sciences*, 36, 531
- de Wijs, G. A., Kresse, G., Vočadlo, L., et al. 1998, *Nature*, 392, 805
- Dumoulin, C., Tobie, G., Verhoeven, O., Rosenblatt, P., & Rambaux, N. 2017, *Journal of Geophysical Research (Planets)*, 122, 1338
- Dziewonski, A. M., & Anderson, D. L. 1981, *Physics of the Earth and Planetary Interiors*, 25, 297
- Florensky, C. P., Ronca, L. B., Basilevsky, A. T., et al. 1977, *Geological Society of America Bulletin*, 88, 1537
- Gelman, A., Roberts, G. O., Gilks, W. R., et al. 1996, *Bayesian statistics*, 5, 42
- Grimm, R. E., & Solomon, S. C. 1988, *J. Geophys. Res.*, 93, 11911
- Harada, Y., Goossens, S., Matsumoto, K., et al. 2014, *Nature Geoscience*, 7, 569
- Harada, Y., Goossens, S., Matsumoto, K., et al. 2016, *Icarus*, 276, 96
- Huang, J., Yang, A., & Zhong, S. 2013, *Earth and Planetary Science Letters*, 362, 207
- James, P. B., Zuber, M. T., & Phillips, R. J. 2010, in *Lunar and Planetary Science Conference*, 41, 2663
- Kaula, W. M. 1979, *Geophys. Res. Lett.*, 6, 194
- Khan, A., Liebske, C., Rozel, A., et al. 2018, *Journal of Geophysical Research (Planets)*, 123, 575
- Knapmeyer, M. 2011, *Planet. Space Sci.*, 59, 1062
- Konopliv, A. S., Banerdt, W. B., & Sjogren, W. L. 1999, *Icarus*, 139, 3
- Konopliv, A. S., Park, R. S., & Folkner, W. M. 2016, *Icarus*, 274, 253
- Konopliv, A. S., & Yoder, C. F. 1996, *Geophys. Res. Lett.*, 23, 1857
- Ksanfomaliti, L. V., Zubkova, V. M., Morozov, N. A., & Petrova, E. V. 1982, *Soviet Astronomy Letters*, 8, 241
- Li, Q., Xue, C., Liu, J.-P., et al. 2018, *Nature*, 560, 582
- Lodders, K., Fegley, B., Lodders, F., et al. 1998, *The Planetary Scientist's Companion* (Oxford University Press on Demand)
- Matsumoto, K., Yamada, R., Kikuchi, F., et al. 2015, *Geophys. Res. Lett.*, 42, 7351
- Mocquet, A., Rosenblatt, P., Dehant, V., & Verhoeven, O. 2011, *Planet. Space Sci.*, 59, 1048
- Mosegaard, K., & Tarantola, A. 1995, *J. Geophys. Res.*, 100, 12431
- Padovan, S., Margot, J.-L., Hauck, S. A., Moore, W. B., & Solomon, S. C. 2014, *Journal of Geophysical Research (Planets)*, 119, 850
- Parmentier, E. M., & Hess, P. C. 1992, *Geophys. Res. Lett.*, 19, 2015
- Peltier, W. R. 1974, *Reviews of Geophysics and Space Physics*, 12, 649
- Saito, M. 1974, *Journal of Physics of the Earth*, 22, 123
- Seidelmann, P. K., Archinal, B. A., A'Hearn, M. F., et al. 2007, *Celestial Mechanics and Dynamical Astronomy*, 98, 155
- Spohn, T., Breuer, D., & Johnson, T. 2014, *Encyclopedia of the Solar System* (Elsevier)
- Steinberger, B., Werner, S. C., & Torsvik, T. H. 2010, *Icarus*, 207, 564
- Stevenson, D. J., Cutts, J. A., Mimoun, D., et al. 2015, *Probing the Interior Structure of Venus* (Keck Institute for Space Studies)
- Takeuchi, H., & Saito, M. 1972, *Methods in Computational Physics*, 11, 217
- Taylor, F. W. 1985, *Geophysical Surveys*, 7, 385
- Williams, J. G., & Boggs, D. H. 2015, *Journal of Geophysical Research (Planets)*, 120, 689
- Xia, Y. F., & Xiao, N. Y. 2002, *Earth Moon and Planets*, 88, 75
- Yang, A., Huang, J., & Wei, D. 2016, *Planet. Space Sci.*, 129, 24
- Yoder, C. F. 1995, *Icarus*, 117, 250
- Zhang, C. Z., & Zhang, K. 1995, *Earth Moon and Planets*, 69, 237